Vol 14 No 1, January 2005
1009-1963/2005/14(01)/0201-07

Chinese Physics

© 2005 Chin. Phys. Soc.
and IOP Publishing Ltd

Resonant tunnelling in parabolic quantum well structures under a uniform transverse magnetic field*

Gong Jian(宫 箭)[a)†], Liang Xi-Xia(梁希侠)[a)b)], and Ban Shi-Liang(班士良)[a)b)]

[a)] *Department of Physics, College of Sciences and Technology, Inner Mongolia University, Hohhot* 010021, *China*

[b)] *CCAST (Word Laboratory), Beijing* 100080, *China*

(Received 28 May 2004; revised manuscript received 16 September 2004)

The resonant tunnelling through parabolic quantum well structures under a uniform transverse magnetic field is investigated by a simple numerical method. Numerical results of the transmission coefficient are obtained for several GaAs–$Al_xGa_{1-x}As$ parabolic well structures. It is found that the resonant peaks shift towards the higher energy region as the magnetic field increases, and some new resonant peaks emerge when the magnetic field becomes stronger. The $J-V$ characteristics of a parabolic quantum well are discussed for the cyclotron centre located at different positions. It is also found that the cyclotron centre located at the parabolic well centre is helpful to explain the experiment, and the peak current densities decrease and shift to higher bias with the increase of magnetic field. The influence of mixed crystal effect on the $J-V$ characteristic under a uniform transverse magnetic field is also investigated.

Keywords: resonant tunnelling, parabolic quantum well, transverse magnetic field
PACC: 7320D, 7340G

1. Introduction

Since Tsu and Esaki[1] investigated the electronic resonant tunnelling through multiple barriers theoretically and observed the negative differential conductance in experiment,[2] the tunnelling through lower-dimensional heterostructures has attracted considerable interest and has been widely investigated both theoretically and experimentally.[3−18]

During the past years, much attention has been focused on the resonant tunnelling in rectangular barrier heterostructures.[3−7] Magneto-tunnelling has been proven to be a powerful tool to study the dynamics of electrons in heterostructures. The tunnelling through multi-layered structures of semiconductors in the parallel electric and magnetic fields along the growth direction has been studied by a number of authors.[8−16] The regular field-induced features or steps in the $I(V)$ curve have been observed.[8,9] In the parallel field case, the Hamiltonian of a system can be separated into an "electric" part giving rise to subbands and a "magnetic" part leading to the Landau levels. Otherwise, the tunnelling problems in a transverse magnetic field normal to the growth direction are more complicated theoretically because of the non-conservation of the transverse components for the electronic momentum. Zaslavsky *et al*[11] and Davies *et al*[12] experimentally observed that the transverse magnetic field shifts the resonant current peaks in the $I(V)$ curve to higher bias positions. The phenomenon is explained by invoking the magnetic-field-induced change in the transverse momentum of the electrons tunnelling into the well.

Ancilato[15] discussed the effect of a transverse magnetic field on the tunnelling in a double-square-barrier structure (DSBS) and gave a numerical solution of one-dimensional (1D) effective mass equation by using the Wentzel–Kramers–Brillouin (WKB) approximation. Some authors investigated the quantum magneto-transport of electrons in a double-barrier resonant structure.[16] They solved the 1D effective mass equation analytically by using Hermitian functions as envelope functions, and calculated the transmission coefficient (TC) for electron tunnelling by the transfer-

*Project supported partly by the National Natural Science Foundation of China (Grant No 10164003) and the Foundation for University Key Teachers by the Ministry of Education (Grant No GG-140-10126-1005).

†E-mail: ndgong@imu.edu.cn

matrix method. The calculated results affirmed that the structure parameters of the systems strongly affect the resonant tunnelling properties. In their calculation the cyclotron centre was chosen fixed at the incident edge of the DSBS. This assumption may not match the experimental situation completely, and further calculations by choosing different locations of the cyclotron centre are needed to understand fully the transverse magnetic field effects on the tunnelling.

At present, the parabolic quantum well (PQW) has been widely investigated and some new properties of electrons in this kind of system are obtained.[19−21] However, the magneto-tunnelling through PQWs under a transverse magnetic field has not been discussed sufficiently. In this paper, we study the resonant tunnelling through a PQW structure under crossed magnetic and electric fields. The one-dimensional Schrödinger equation for this case is solved by using a simple numerical method, which has been developed to study the electronic tunnelling without a magnetic field,[6,22] and to calculate the transmission coefficients and wavefunctions of electrons with variable effective mass across several GaAs–$Al_xGa_{1-x}As$ PQW structures. It is found that the resonant peaks shift to higher energy region with the increase of magnetic field for both zero and non-zero bias voltages, and also some new resonant peaks emerge under a much stronger transverse magnetic field. The $J-V$ characteristics are discussed for the cyclotron centre located at the different positions. We also found that the cyclotron centre located at the centre of the parabolic well instead of being fixed at other positions[15,16] is more helpful to explain the experiment. The current peaks shift to higher bias and the peak current becomes weaker with increasing magnetic field. The influence of mixed crystal effect on the $J-V$ characteristic under a uniform transverse magnetic field is also investigated.

2. Theoretical model

Consider a PQW tunnelling structure grown in the z-direction, whose potential the electrons undergone can be divided into three regions: the region II constructs a PQW of width l with finite barriers, and in the other regions of the space I ($z \leqq -l/2$) and III ($z \geqq l/2$) the electrons are free and the potential is chosen as zero. The solid line in Fig.1 schematically illustrates the parabolic-well potential profile without bias and magnetic field. We assume a uniform magnetic field is supplied in the x-direction, i.e. $\vec{B} = (B, 0, 0)$. In the emitter and collector regions ($|z| \geqq l/2$), the coherence of the Landau motion is destroyed by the ionized impurity scattering so that the magnetic-field effect is small enough to be ignored. Thus the vector potential can be chosen as $\vec{A} = (0, -Bz, 0)$ in the system and $\vec{A} = 0$ out of the system in the Landau gauge.

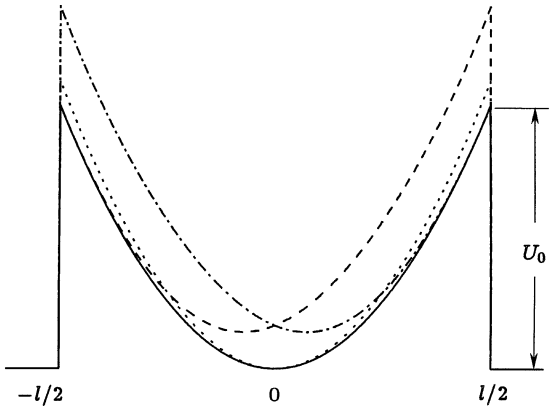


Fig.1. Schematic illustration of PQW resonant tunnelling structure. The solid line is for $B = 0$, the dashed line, the dotted line and the dot-dashed line are for $B \neq 0$ and $z_0 = -l/2, 0$, and $l/2$, respectively.

2.1. Transmission coefficients T (E, V, B, z_0)

The Schrödinger equation for an electronic motion in the system is then written as

$$\left[\frac{P_x^2}{2m^*(z)} + \frac{1}{2}P_z\frac{1}{m^*(z)}P_z + \frac{1}{2m^*(z)}\left(P_y - eBz\right)^2 + U\left(z\right) - eFz\right]\Psi(\vec{r}) = E\,\Psi(\vec{r}). \tag{1}$$

In Eq.(1), $U(z)$ is the potential and can be written as

$$U\left(z\right) = \begin{cases} U_0 z^2 \Big/ \left(\dfrac{l}{2}\right)^2, & -\dfrac{l}{2} < z < \dfrac{l}{2} \\ 0, & z \leq -\dfrac{l}{2} \ \text{ or } \ z \geq \dfrac{l}{2} \end{cases} \tag{2}$$

where l is the width of the well. $m^*(z)$ is the variable effective mass of the electron. F is the electric field strength, and E is the total energy of the electrons. Considering the transverse symmetry in the $x-y$ plane, we choose the wavefunction $\Psi(\vec{r})$ in Eq.(1) in the following form:

$$\Psi(\vec{r}) = \varphi\left(z\right)\exp\left(\mathrm{i}k_x x + \mathrm{i}k_y y\right), \tag{3}$$

where $\varphi(z)$ is the wavefunction describing the electron tunnelling along the parabolic well of z-direction.

Substituting Eq.(3) into Eq.(1), we obtain

$$-\frac{\hbar^2}{2}\frac{\partial}{\partial z}\frac{1}{m^*(z)}\frac{\partial}{\partial z}\varphi(z) + \left[\frac{1}{2}m^*(z)\,\omega_c^2(z)\,(z-z_0)^2 + U(z) - eFz\right]\varphi(z) = \left[E - \frac{\hbar^2 k_x^2}{2m^*(z)}\right]\varphi(z), \quad (4)$$

where $z_0 = l_B^2 k_y$ is the so-called "cyclotron centre" in the z-direction related to the wavevector component k_y of the electronic transverse motion, and the parameter $l_B = (\hbar/eB)^{1/2}$ depends on the magnetic field. The cyclotron frequency is determined by

$$\omega_c(z) = \frac{eB}{m^*(z)}. \quad (5)$$

Defining an effective potential

$$U_{\text{eff}}(z,B) = \frac{1}{2}m^*(z)\,\omega_c^2(z)\,(z-z_0)^2 + U(z) - eFz, \quad (6)$$

and neglecting the thermal motion of the electron in the x-direction by choosing $k_x = 0$, the Schrödinger equation can be reduced to

$$-\frac{\hbar^2}{2}\frac{\mathrm{d}}{\mathrm{d}z}\frac{1}{m^*(z)}\frac{\mathrm{d}}{\mathrm{d}z}\varphi(z) + U_{\text{eff}}(z,k_y,B)\,\varphi(z) = E\varphi(z). \quad (7)$$

The electronic wavefunctions $\varphi(z)$ in regions I, II and III can be written respectively as[6]

$$\varphi_1(z) = A_1 \mathrm{e}^{\mathrm{i}k_1 z} + B_1 \mathrm{e}^{-\mathrm{i}k_1 z}, \quad (8)$$

$$\varphi_2(z) = A_2 f(z) + B_2 g(z), \quad (9)$$

$$\varphi_3(z) = A_3 \mathrm{e}^{\mathrm{i}k_3 z}, \quad (10)$$

where

$$k_i = \frac{1}{\hbar}\sqrt{2m^*(z)(E - U_{\text{eff}}(z,B))} \quad (i = 1,2,3).$$

According to the continuity of $\varphi_i(z)$ and $(1/m^*(z))\,\mathrm{d}\varphi_i(z)/\mathrm{d}z$ at every boundary, the coefficients in Eqs.(8)–(10) should satisfy the following relation:

$$\begin{bmatrix} A_1 \\ B_1 \end{bmatrix} = \begin{bmatrix} t_{11} & t_{12} \\ t_{21} & t_{22} \end{bmatrix} \begin{bmatrix} A_3 \\ 0 \end{bmatrix}. \quad (11)$$

The transmission coefficient T is determined by

$$T = \left|\frac{1}{t_{11}}\right|^2 \frac{k_3}{k_1}. \quad (12)$$

The functions $f(x)$ and $g(x)$ in Eq.(9) can be solved numerically by the well-known Runge–Kutta method.

2.2. Current density-voltage characteristic of PQWs

The scattering due to phonons and impurities can be neglected as an approximation since we focus our attention on the electron tunnelling and the influence of bias voltage V and magnetic field B for a GaAs–$Al_xGa_{1-x}As$ system. Furthermore, we ignore any inter-band tunnelling which may occur for a high bias voltage, when the quasi-Fermi level of the collector is located below the valence-band maximum of the bulk emitter. Within the single-electron approximation, the equation of tunnelling current density from emitter to collector is written as[1]

$$J = \frac{e}{4\pi^3\hbar}\int_0^\infty \mathrm{d}k_z \int_0^\infty \mathrm{d}\vec{k}_{//} \times [f_{\text{emitter}}(E,V) - f_{\text{collector}}(E,0)] \times T(E_z,V,B)\frac{\partial E}{\partial k_z}, \quad (13)$$

where $f(E,V) = 1/(1+\mathrm{e}^{(E-E_f+eV)/k_BT})$ is the Fermi function. Equation (13) can be simplified to

$$J = \frac{em_E^* k_B T}{2\pi^2\hbar^2}\int_0^\infty \mathrm{d}E_z T(E_z,V,B) \times \ln\left(\frac{1+\mathrm{e}^{(E_f-E_z)/k_BT}}{1+\mathrm{e}^{(E_f-E_z-eV)/k_BT}}\right), \quad (14)$$

where m_E^* is the effective mass in the emitter, E_f and k_B are the Fermi energy and Boltzmann constant respectively.

3. Numerical calculation and discussion

The numerical calculations have been carried out for three types of parabolic wells consisting of GaAs–$Al_xGa_{1-x}As$ system. The well of type A has a narrow width l of 10nm and U_0=0.9587eV. For type B the well width is 22nm and U_0=0.3eV. For type C, we choose l= 16nm and U_0=0.4655eV. The conduction band offset U_0 and the effective mass $m^*(z)$ in the parabolic wells are determined as functions of aluminium content x by the following equation:

$$U_0 = \begin{cases} 0.75x \ \text{eV} & (0 \le x \le 0.45), \\ 0.75x + 0.69(x-0.45)^2 \ \text{eV} & (0.45 \le x \le 1), \end{cases} \quad (15)$$

$$m^*(z) = 0.067 + 0.083x \quad (0 \le x \le 1). \quad (16)$$

The calculated transmission coefficients (TCs) as functions of electronic energy in the zero bias case for types A and B are shown in Figs.2 and 3 respectively,

where the cyclotron centre is located at the incident edge of the parabolic wells. It is clearly seen that the resonant peaks shift toward the higher energy region with the increase of magnetic field. It is also found from Figs.2 and 3 that the maximum of TC almost equals unity for type A, whose well potential is narrow and high in a stronger magnetic field. Otherwise, the maximum of TC is much lower than unity as the magnetic field increases for type B. The magnetic field influences the TC in two respects. First, the transverse magnetic field heightens the potential barriers so that the electron energy levels rise up. Second, it breaks the symmetric property of the effective potentials in tunnelling structures if the cyclotron centre is not located at the well centre. Since $z_0 = l_B^2 k_y$, the cyclotron centre is determined from the electronic transverse wavevector k_y. The degree of broken symmetry is determined by the magnetic field strength and the structure parameters. This is the reason why the asymmetric property is more remarkable in the PQW tunnelling structure for Fig.3 than that for Fig.2. As a result, the increase of magnetic field will decrease the maximum of TC. However, if the electronic transverse motion makes the cyclotron centre be located at the centre of parabolic well, the transverse magnetic field will no longer break the symmetry of the structures, so that the maximum of resonant peaks is always equal to unity. The detailed result is given in Fig.4, which shows the TC as a function of electron energy for type B structure with the cyclotron centre located at the centre of the parabolic well. It is found that the maximum of TC still remains unity with the increase of magnetic field.

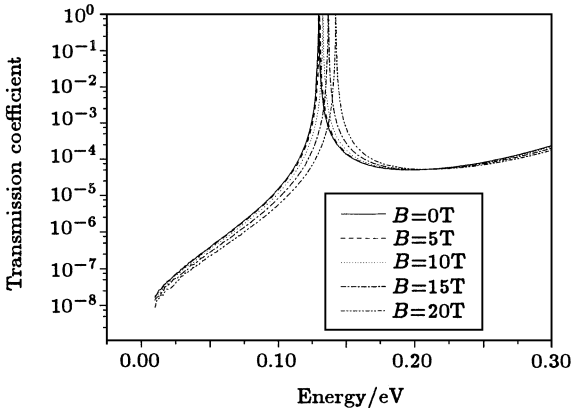


Fig.2. Transmission coefficient T as a function of electron energy E in type A structure without a bias. The cyclotron centre is located at the incident edge of the effective potential.

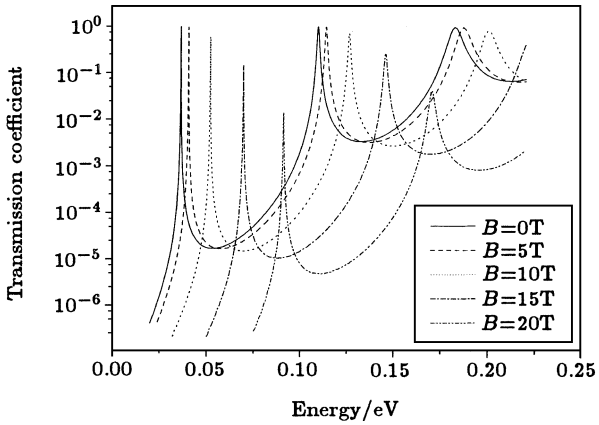


Fig.3. Transmission coefficient T as a function of electron energy E in type B structure without a bias. The cyclotron centre is located at the incident edge of the effective potential.

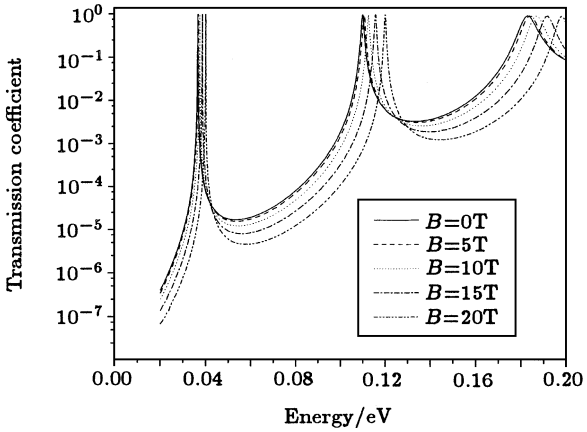


Fig.4. Transmission coefficient T as a function of electron energy E in type B structure without a bias. The cyclotron centre is located at the centre of the effective potential.

The 3D plot of TC as a function of magnetic field B and electron energy E with a bias voltage $F = 2.5 \times 10^2$kV/cm is shown in Fig.5 for type C structure. A novel result is obtained that the resonant peaks shift towards the higher energy region with increasing magnetic field B. Furthermore, some new resonant peaks emerge when the magnetic field becomes much stronger. It is easily comprehended since the magnetic field lifts the electronic energy levels in the well, and some energy levels below the conduction band will emerge with the increase of magnetic field.

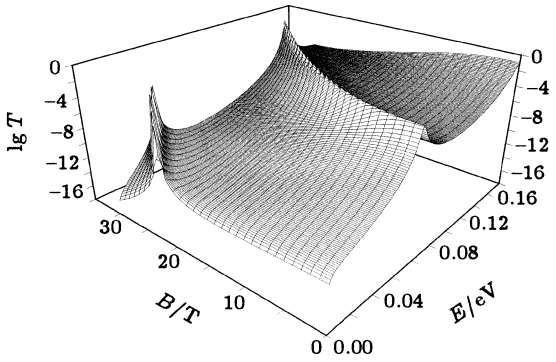


Fig.5. Transmission coefficient T as a function of electron energy E and transverse magnetic field B in type C structure with the bias voltage $F = 2.5\times10^2$kV/cm.

The $J-V$ characteristics of resonant tunnelling in a PQW for type C structure under different transverse magnetic fields are calculated and the results are presented in Fig.6. For understanding the transverse magnetic effect on the tunnelling in the system clearly, we have chosen the cyclotron centre at three different positions, the incident edge, the centre and the collector edge of the PQW tunnelling structure. In the previous calculations for the DSBS,[16] the cyclotron centre was chosen located at the incident edge of the system. The results affirmed that the peaks of tunnel current shift to higher voltage and the tunnelling currents are weakened with increasing transverse magnetic field in a square well system. Different from Ref.[16], our calculated results for the same situation show in Fig.6(a) that the resonant peaks also shift to higher voltages, but the current densities are raised instead of reduced with increasing magnetic field. Otherwise, when the cyclotron centre is located at the collector edge of PQW structure ($z_0 = l/2$), the resonant peaks shift to higher bias and the currents are reduced rapidly with the increase of the transverse magnetic field (see Fig.6(c)). It is understood that the transverse magnetic field supplies an added potential to U_{eff} and raises the barriers of the PQW (see Fig.1), so that the energy of the resonant state rises and then the resonant peaks shift to the higher biases. Figure 1 shows the magnetic contributions to U_{eff} for the cases of $z_0 = -l/2, l/2$ and 0 without the bias. The magnetic field raises the barriers of the emitter edge for $z_0 = -l/2$, the collector edge for $z_0 = l/2$ and both for $z_0 = 0$ respectively. When a bias is added, the effective potential is no longer symmetric and the peak of the transmission probability is no longer 1 even for B=0. However, in $z_0 = -l/2$ case for $B \neq 0$, the magnetic field raises the collector barrier and makes the effective potential nearer symmetric and the transmission easy. Therefore, the current density is also enhanced compared with that in B=0 case. The incident barrier rises and the collector barrier falls so that the peaks of the tunnelling current drops with the cyclotron centre moving from $-l/2$, to $l/2$. In fact, the position of the cyclotron centre depends on the y-component of the electron wave-vector, which should be considered to be varying between the values corresponding to $z_0 = -l/2$ and $z_0 = l/2$ in the calculation of the tunnelling current. So the calculation of the tunnelling current by fixing the cyclotron centre at either $z_0 = -l/2$ (the incident edge) or $z_0 = l/2$ (the collector edge) may not give a correct result. A reasonable choice is to fix the cyclotron centre at the average position, i.e. the centre of the PQW structure (z_0=0). This calculation presents an average effect, which can be observed in experiment. The results shown in Fig.6(b) are in qualitative agreement with the magnetic-field effects observed in experiment for a square quantum well.[11−14] It is found that the current peaks shift to the higher bias, the resonant peaks are broadened, and the peak currents are a little weakened.

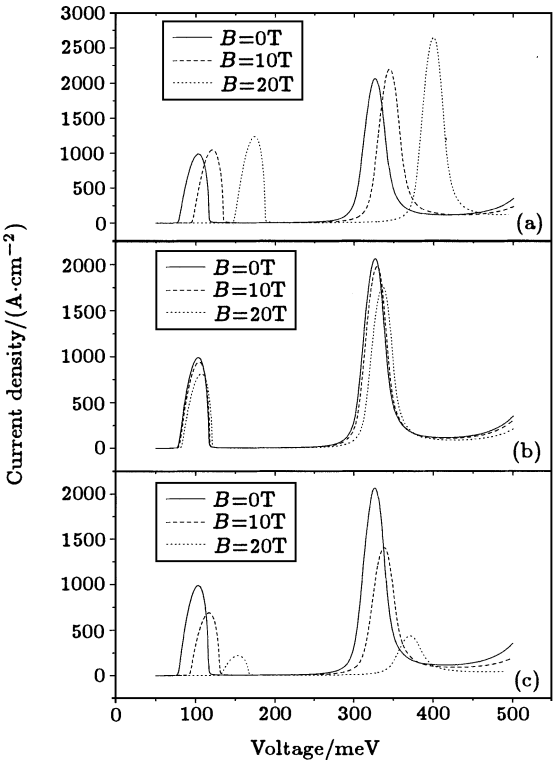


Fig.6. Current density versus applied voltage at T=4.2K for (a) the cyclotron centre located at the incident edge of parabolic well; (b) the cyclotron centre located at the centre of parabolic well; (c) the cyclotron centre located at the collector edge of parabolic well.

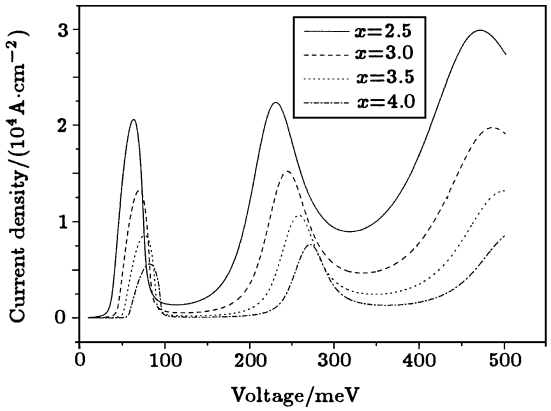


Fig.7. Current densities versus applied voltage for a parabolic well under a magnetic field B=10T corresponding to aluminium content x=0.25, 0.3, 0.35, 0.4.

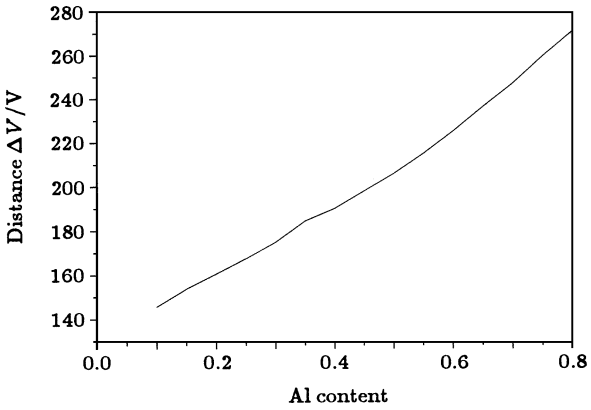


Fig.8. The distance between the first and the second current peak positions versus aluminium content under a magnetic field B=10T.

The ternary mixed crystal effect on the tunnelling characteristic is shown in Figs.7 and 8. The $J-V$ curves under a magnetic field B=10T are plotted in Fig.7 corresponding to different aluminium content of ternary mixed crystals $Al_xGa_{1-x}As$ at the edge of tunnelling structure with x=0.25, 0.3, 0.35, 0.4. It is found that the current peaks are rapidly weakened and shift to higher bias with the increase of x and the barrier height reduces. Finally, we consider the influence of mixed crystal effect on the position of current peaks. For this purpose, we plot the distance between the first and the second current peak positions as a function of x under the magnetic field B=10T in Fig.8. It is seen that the distance increases obviously with increasing x. The results in Figs.7 and 8 can be easily understood from the fact that the shape of parabolic well can be adjusted by changing the aluminium content in the ternary mixed crystal $Al_xGa_{1-x}As$. With increasing x, the shape of the parabolic potential becomes cliff-like and the barriers are heightened to block the penetration of electrons.

4. Conclusions

We have investigated the effect of crossed uniform transverse magnetic and electron fields on the resonant tunnelling in GaAs-$Al_xGa_{1-x}As$ parabolic well structures by using a simple numerical method. It is found that the transverse magnetic field supplies an additional potential and raises the barriers of the PQW (see Fig.1), so that the resonant peaks shift to higher biases. Different localizations of the centre of the cyclotron motion built by the applied transverse magnetic field produce different qualitative results for the transmission coefficient and tunnelling current. An average choice to locate the cyclotron centre at the centre of the parabolic well is reasonable to do the calculations and explain experimental result correctly. The resonant peaks shift to higher energies when the bias is applied. Furthermore, some new peaks emerge when the magnetic field becomes much stronger. It is indicated that the effects of electron transverse motion and structure parameters cannot be neglected; the role of magnetic and electric fields is important for resonant tunnelling. The $J-V$ characteristics of resonant tunnelling under different magnetic fields are investigated. It is shown that the current peaks shift to the higher bias and become weaker with increasing magnetic field. Meanwhile the influence of mixed crystal effect on current density is also significant so that the peak currents are rapidly weakened with the increase of Al content. This result is useful in the application of PQW structure.

Acknowledgements

S. L. Ban and J. Gong acknowledge the support of the 111 and 321 Projects of Inner Mongolia Autonomous Region, China.

References

[1] Tsu R and Esaki L 1973 *Appl. Phys. Lett.* **22** 562

[2] Chang L L, Esaki L and Tsu R 1974 *Appl. Phys. Lett.* **24** 593

[3] Ando Y and Itoh T 1987 *J. Appl. Phys.* **61** 1497

[4] Boykin T B 1995 *J. Appl. Phys.* **78** 6818

[5] Wang X H, Gu B Y and Yang G Z 1997 *Phys. Rev.* B **55** 9340

[6] Ban S L, Hasbun J E and Liang X X 2000 *J. Luminescence.* **87–89** 369

[7] Duschi R, Scharidt O G and Eberl K 2000 *Appl. Phys. Lett.* **76** 879

[8] Zaslavsky A, Tsui D C, Santos M and Shayegan M 1989 *Phys. Rev.* B **40** 9829

[9] Leadbeater M L, Alves E S, Eaves L, Henini M *et al* 1989 *Phys. Rev.* B **39** 3438

[10] Yan Z W and Liang X X 2002 *Phys. Rev.* B **66** 235324

[11] Zaslavsky A, Yuan P, Tsui D C, Santos M and Shayegan M 1990 *Phys. Rev.* B **42** 1374

[12] Davies R A, Newson D J, Powell T G, Kelly M J and Myron H W 1987 *Semicond. Sci. Technol.* **2** 61

[13] Helm M, Peeters F M, England P, Hayes J R and Colars E 1989 *Phys. Rev.* B **39** 3427

[14] Peeters F M, Helm M, England P, Hayes J R, Colas E, Harbison J P and Florez L T 1989 *Solid State Electron.* **32** 1309

[15] Ancilotto F 1988 *J. Phys.* C **21** 4677

[16] Guo Y, Li Y C, Kong X J and Wei C W 1994 *Phys. Rev.* B **50** 17249

[17] Xie Z W and Li B Z 2002 *Acta Phys. Sin.* **51** 399

[18] Luo X D, Bian L F, Xu Z Y *et al* 2003 *Acta Phys. Sin.* **52** 1761

[19] Miller R C, Gossard A C, Kleinman D A and Munteau O 1984 *Phys. Rev.* B **29** 3740

[20] Hai G Q and Peeters F M 1999 *Phys. Rev.* B **60** 8984

[21] Zhao F Q, Liang X X and Ban S L 2003 *Eur. Phys. J.* B **33** 3

[22] Gong J, Ban S L and Liang X X 2002 *Int. J. Mod. Phys.* B **16** 4607